Performance Analysis of an OFDMA Transmission System in a Multi-Cell Environment

Sophie Gault, Walid Hachem(*), and Philippe Ciblat

Abstract

The paper deals with design and performance analysis of Orthogonal Frequency Division Multiple Access (OFDMA) based downlink cellular wireless communications. Due to a high degree of users mobility, the Base Station is assumed to have only a statistical knowledge of the users channels. Relying on the ergodic capacities connected to the user rates, a sub-carrier and power allocation that minimizes the total transmitted power is proposed. The allocation strategy requires only the knowledge of the channel statistics and the rate requirements for all users. An extension and a performance analysis of this allocation algorithm in a multi-cell environment working with a frequency re-use factor equal to one is also conducted. A condition for the multi-cell network to be able to satisfy all rate requirements is derived.

Index Terms

Ergodic Capacity, Frequency Hopping, Multi-Cell Interference, OFDMA, Power and Sub-Carrier Allocation.

I. Introduction

In wireless multi-user communications, Orthogonal Frequency Division Multiple Access (OFDMA) is a technique that combines discrete multi-carrier modulation with a frequency division multiple access

(*) Corresponding author.

Sophie Gault (sophie.gault@motorola.com) and Walid Hachem (w.hachem@ieee.org) were with Supélec, Telecommunications Department, Plateau de Moulon, 91192 Gif-sur-Yvette, France. Philippe Ciblat (philippe.ciblat@enst.fr) is with Ecole Nationale Supérieure des Télécommunications (ENST), Département Communications et Electronique, 46, rue Barrault, 75013 Paris, France.

based on the dynamic allocation of sub-carriers to users. The advantages of OFDMA include the flexibility in sub-carrier attribution, the absence of multi-user interference due to sub-carrier orthogonality, and the simplicity of the receiver. An OFDM modulation associated with a Frequency-Hopping (FH) multiple access technique can be also viewed as a spread spectrum technique. Consequently FH-OFDMA offers the advantage of averaging interference as in a CDMA system and thus enables us to construct a cellular network with a frequency re-use factor between the adjacent cells equal to one [1], [2]. Thanks to these advantages, OFDMA receives a great deal of attention as a candidate for future wireless communication standards. Yet, the problem of the optimum sub-carrier and power attribution to users as well as the robustness of OFDMA to inter-cell interference in a multi-cell setting are not fully understood. This paper is a contribution toward solving these problems for downlink communications.

The power and sub-carrier allocation problem for OFDMA has been addressed by a number of contributions, among which [3]–[9] can be cited. These contributions assume the transfer functions of all users channels as being known to the Base Station (BS). In a multi-cell setting, [10], [11] propose solutions that involve coordination between Base Stations through the existence of a radio network controller that gathers all channels state information in order to solve globally the sub-carrier allocation problem. In this paper, we assume that these transfer functions are not available at the BS due to a high degree of users mobility, and for computational complexity reasons, that Base Stations do not cooperate. Assuming that the channels are random and frequency selective and that the BS has only a statistical knowledge of these channels, the general problem that we address is the following: given the data rates required by the users, the BS has to find the optimum number of sub-carriers and power per user in such a way that the rate requirements of all users are satisfied and at the same time the total transmitted power is minimum. Due to the time and frequency diversity of the users channels and to the non availability of the channels transfer functions at the BS site, we consider that a relevant measure of the achievable rate between the BS and a user is the so-called ergodic capacity. In practice, through frequency hopping, the signal sent to a given user within a data frame visits a large number of this user's channel states and benefits from an averaging effect over the corresponding gains. This justifies the use of ergodic capacity as a performance measure.

One advantage of minimizing the BS transmitted power is to mitigate the interference that disturbs the neighboring cells. Nevertheless, this so-called Multi-Cell Interference (MCI) still represents a fundamental obstacle against a possible increase of the whole cell capacity. In the second part of the paper, we analyze thoroughly the impact of Multi-Cell Interference over the system performance. For a BS of interest, a simple way to combat the MCI that comes from the neighboring cells, is to increase its own transmitted power. Consequently, in turn, the neighboring Base Stations will also have to increase their powers. If the system is to work, this process should converge. This leads to the issue of the whole system stability. In order to be able to conduct our performance analysis under the presence of MCI, and in particular, to derive a condition for the system stability, we begin by assuming that the number of users in a cell and the signal bandwidth grow both toward infinity in such a way that the total rate (or capacity) of the BS per channel use[1] converges toward a constant. A parameter of prime importance will emerge from our analysis : this is the mean rate per channel use and per cell volume unit required by the users in a cell. By considering an idealized network where all cells are identical and regularly spaced, we show that the network is stable if this rate is less than a given threshold. An analysis of this threshold in terms of certain system parameters like the cell radius and the power decay profile will also be conducted.

In section II, we state the allocation problem for the single cell case. Section III is devoted to the solution of the power and sub-carrier optimization problem, that shows to be solvable by means of a Lagrangian formulation. The asymptotic regime in the number of users introduced above is described rigorously in section IV. Under this regime, the issues of performance in presence of MCI and network stability are addressed in section V. Finally, section VI is devoted to the numerical illustrations of the results. We also compare the multi-cell OFDMA approach with an OFDMA technique assigning different sets of sub-carriers to adjacent cells and thus working with a frequency re-use factor less than one.

In the paper, $\mathbb{E}[.]$ will denote the expectation operator. The (multivariate) complex-valued circular Gaussian distribution with mean $\mathbf{a}$ and covariance matrix $\mathbf{\Sigma}$ will be denoted $\mathcal{CN}(\mathbf{a}, \mathbf{\Sigma})$.

II. Single Cell Model

We consider a downlink transmission where a BS serves K users. The users channels are time varying frequency selective channels. The transmitted signal is parsed into frames, each corresponding to an OFDM (Orthogonal Frequency Division Multiplexing) symbol of duration T seconds. The channel impulse response of user k, assumed invariant during OFDM symbol m, is represented during this symbol by the vector $\mathbf{h}_k(m) = [h_k(m,0), \ldots h_k(m,L-1)]^{\mathrm{T}}$ where L is an upper bound on the users channel lengthes. Denoting by N the number of sub-carriers in an OFDM symbol (equivalently the number of channel uses per OFDM symbol), let $\mathbf{H}_k(m) = [H_k(m,0), \ldots, H_k(m,N-1)]^{\mathrm{T}}$ be the vector that represents the transfer function of the channel of user k at the N Fourier frequencies of OFDM symbol m. In other words, $\mathbf{H}_k(m) = \sqrt{N}\mathbf{F}_{N,L}\mathbf{h}_k(m)$ where $\mathbf{F}_{N,L}$ is the $N \times L$ Fourier matrix which (n,l)

[1]The capacity per channel use is the capacity divided by the channel bandwidth

entry is given by $[\mathbf{F}]_{n,l} = \frac{1}{\sqrt{N}} \exp\left(-2i\pi nl/N\right)$ for $n = 0, \ldots, N-1$ and $l = 0, \ldots, L-1$. The signal $Y_k(m,n)$ received by user k at sub-carrier n after the Discrete Fourier Transformation of OFDM symbol m writes then

$$Y_k(m,n) = H_k(m,n)S(m,n) + V_k(m,n) \tag{1}$$

where $S(m,n)$ is the signal transmitted by the BS in the discrete Fourier domain and $V_k(m,n)$ is the additive noise received by user k at sub-carrier n of OFDM symbol m. We assume that the two dimensional noise process $V_k(m,n)$ is white, and that a sample of this process has the distribution $\mathcal{CN}(0,\sigma^2)$ where σ^2 refers to the noise variance. Recall that this variance is written as $\sigma^2 = N_0 B$ where N_0 is the noise Power Spectral Density and $B = N/T$ is the system bandwidth, or equivalently the number of channel uses per second. We formulate the following assumption regarding the users channels:

(A) The vector process $\mathbf{h}_k(m)$ is a random process with distribution $\mathcal{CN}(\mathbf{0}, \mathbf{\Sigma}_k)$ where

$$\mathbf{\Sigma}_k = \begin{bmatrix} \varsigma_{k,0}^2 & & 0 \\ & \ddots & \\ 0 & & \varsigma_{k,L-1}^2 \end{bmatrix} .$$

Assumption (A) states that the channel taps in the time domain are circular Gaussian and independent but they do not have necessarily the same variances. A consequence of (A) is that all entries of $\mathbf{H}_k(m)$, *i.e.*, the transfer function coefficients in the discrete Fourier domain, have the distribution $\mathcal{CN}(0, \varsigma_k^2)$ with a variance $\varsigma_k^2 = \sum_{l=0}^{L-1} \varsigma_{k,l}^2$. The fact that they have the same variance ς_k^2 can be verified by inspecting the diagonal elements of the matrix $\mathbb{E}\left[\mathbf{H}_k(m)\mathbf{H}_k^{\mathrm{H}}(m)\right] = N\mathbf{F}_{N,L}\mathbf{\Sigma}_k\mathbf{F}_{N,L}^{\mathrm{H}}$. It results that the "Gain to Noise Ratios" (GNR) $G_k(m,n) = |H_k(m,n)|^2 / N_0$ of user k for $n \in \{0, \ldots, N-1\}$ and $m \in \mathbb{Z}$ are identically distributed.

In the sequel, it will be assumed that the receiver of user k has the knowledge of its channel impulse response and of its noise power. Alternatively, at the BS, only the K mean Gain to Noise Ratios a_k given by

$$a_k = \mathbb{E}\left[G_k(m,n)\right] = \varsigma_k^2 / N_0 \tag{2}$$

are assumed available. With these assumptions, we shall be interested all along this paper in the so-called ergodic Shannon capacities of these channels. Recall that the ergodic capacity can be approached by coding schemes that exploit properly the channel coherence bandwidth and/or its coherence time which we shall assume in the sequel.

In order to state our problem clearly, we begin by assuming that there is only one user ($K = 1$)

communicating with the BS. To be able to reach the capacity, the transmitter has to send independent centered Gaussian signals over the N sub-carriers. In our case, since the random variables $G_k(m,n)$ are identically distributed, the capacity is reached when these Gaussian signals have the same variances. Assume that the user requires a rate of ρ_1 bits per channel use and denote by E_1 the minimum transmitted energy per channel use needed to satisfy this rate requirement. Then E_1 satisfies $\rho_1 = \mathbb{E}\left[\log\left(1+E_1 G_1\right)\right]$ where G_1 is a random variable that has the same probability distribution as any of the random variables $G_k(m,n)$ and the expectation is taken with respect to this random variable. Note that the part of the energy devoted to the guard interval is neglected in this expression.

Let us turn now to the case where $K > 1$. In this paper we restrict ourselves to a sub-optimal user share strategy in information-theoretic point of view. Indeed, we focus on OFDMA scheme which means that for any sub-carrier n and OFDM symbol m, the signal $S(m,n)$ is allocated to a single user. We denote by γ_k the sharing factor associated with user k. The factor γ_k provides the proportion of time-frequency slots (m,n) for which $S(m,n)$ is allocated to user k. By definition, we therefore have $\gamma_k \geq 0$ and $\sum_{k=1}^{K} \gamma_k \leq 1$. Once the sharing factors $\{\gamma_1,\ldots,\gamma_K\}$ are chosen, the practical allocation can be done in several ways: in theory, at one extreme, one can imagine that a user is given a whole OFDM symbol from time to time ; at the other extreme, a user is given some fixed subset of the N sub-carriers of cardinality n_k such that $n_k/N = \gamma_k$ up to a rounding error. In many practical situations, a more reasonable access scheme consists in allocating sub-carriers to users according to some frequency hopping pattern [12]. Here, this pattern will be designed in such a way that constraints associated with the sharing factors γ_k are respected.

Let $E_k = \mathbb{E}\left[|S(m,n)|^2\right]/B$ be the energy transmitted on the sub-carrier n of OFDM symbol m when the slot (m,n) is destined to user k. The ergodic capacity per channel use C_k given to user k is then

$$C_k = \gamma_k \mathbb{E}\left[\log\left(1+\frac{|H_k(m,n)|^2 B E_k}{\sigma^2}\right)\right] = \gamma_k \mathbb{E}\left[\log\left(1+G_k E_k\right)\right] \tag{3}$$

where G_k is a random variable that has the same distribution as $G_k(m,n)$ and the expectation $\mathbb{E}$ is taken with respect to the distribution of G_k. Denoting by Q_k the mean energy per channel use sent to user k, we have $Q_k = \gamma_k E_k$. The mean energy per channel use Q transmitted by the BS is then

$$Q = \sum_{k=1}^{K} Q_k \ . \tag{4}$$

Our problem is then the following : given a rate vector $\boldsymbol{\rho} = [\rho_1,\ldots,\rho_k]^{\mathrm{T}}$ where ρ_k is the capacity per channel use required by user k, find the energies $\{E_k\}$ and the sharing factors $\{\gamma_k\}$ such that the total transmitted energy Q is minimum. Formally, this problem is written : minimize Q with the constraints

$$-C_k + \rho_k \leq 0 \quad \text{for } k = 1, \ldots, K \tag{5}$$

$$\sum_{k=1}^{K} \gamma_k - 1 \leq 0 \ . \tag{6}$$

The capacity C_k given by Equation (3) is not a convex nor a concave function of (γ_k, E_k). However, by writing

$$C_k = \gamma_k \mathbb{E}\left[\log\left(1 + G_k \frac{Q_k}{\gamma_k}\right)\right] \ , \tag{7}$$

it appears that C_k is a concave function of (γ_k, Q_k). Indeed, consider the function $f(x, y) = x \log(1+y/x)$ defined on $\mathbb{R}_+^2$. As the eigenvalues of the 2×2 Hessian matrix associated with $f(x, y)$ are 0 and $-\frac{x^2+y^2}{x(x+y)^2}$, this function is concave. It results that $C_k = \mathbb{E}\left[f\left(\gamma_k, G_k Q_k\right)\right]$ is concave.

In the next section, we will minimize the cost function (4) under the constraints (5-6) by using the Lagrangian multipliers.

III. The Allocation Algorithm

Our constrained minimization problem (5-6) is convex in the vector parameter $\mathbf{x} = \left[\mathbf{q}^{\mathrm{T}}, \boldsymbol{\gamma}^{\mathrm{T}}\right]^{\mathrm{T}}$ where $\mathbf{q} = [Q_1, \ldots, Q_K]^{\mathrm{T}}$ and $\boldsymbol{\gamma} = [\gamma_1, \ldots, \gamma_K]^{\mathrm{T}}$. The Lagrange-KKT conditions are then written

$$\nabla_{\mathbf{x}} Q - \sum_{k=1}^{K} \lambda_k \nabla_{\mathbf{x}} C_k + \beta \nabla_{\mathbf{x}} \left(\sum_{k=1}^{K} \gamma_k\right) = 0 \tag{8}$$

where $\nabla_{\mathbf{x}}$ denotes the gradient operator with respect to the vector $\mathbf{x}$, the positive real numbers $\lambda_1, \ldots, \lambda_K$ are the Lagrange multipliers associated with constraints (5) and the positive number β is the Lagrange multiplier associated with the constraint (6). The multi-variate equation (8) can be rewritten as the set of $2K$ scalar equations $\lambda_k \partial C_k / \partial Q_k = 1$ and $\lambda_k \partial C_k / \partial \gamma_k = \beta$ for $k = 1, \ldots, K$. By developing the left hand members of these Equations, we obtain

$$\lambda_k \mathbb{E}\left[\frac{G_k}{1 + G_k E_k}\right] = 1 \tag{9}$$

$$\lambda_k \mathbb{E}\left[\log\left(1 + G_k E_k\right) - \frac{G_k E_k}{1 + G_k E_k}\right] = \beta \tag{10}$$

for $k = 1, \ldots, K$. By plugging Equations (9) into (10) we have

$$f_1(E_1) = f_2(E_2) = \cdots = f_K(E_K) = \beta \tag{11}$$

where

$$f_k(x) = \frac{\mathbb{E}\left[\log\left(1 + xG_k\right) - \frac{xG_k}{1+xG_k}\right]}{\mathbb{E}\left[\frac{G_k}{1+xG_k}\right]} = \frac{\mathbb{E}\left[\log\left(1 + xG_k\right)\right]}{\mathbb{E}\left[\frac{G_k}{1+xG_k}\right]} - x \ . \tag{12}$$

Let us inspect the middle member of this expression. For every $a > 0$, the function $g_a(x) = \log(1 + ax) - ax/(1 + ax)$ increases from zero to infinity as x increases from zero to infinity. Therefore, the numerator increases from zero to infinity with x. As the denominator decreases with x, the function $f_k(x)$ increases from zero to infinity over the interval $[0, \infty)$ as shown on figure 1. The allocation algorithm

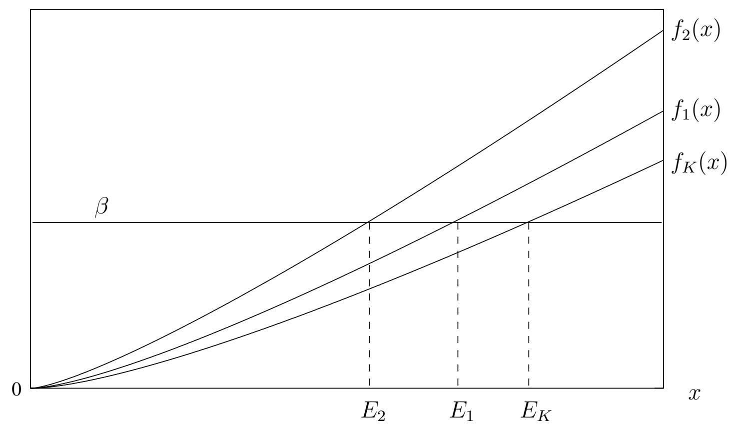

Fig. 1. Shapes of functions $f_k(x)$ and evolution of energies vs β

is the following: initialize β to a value close to zero. Compute the energies E_k by solving numerically Equations (11). To obtain the rate ρ_k, user k needs the sharing factor $\gamma_k(\beta)$ given by

$$\gamma_k(\beta) = \frac{\rho_k}{\mathbb{E}\left[\log\left(1 + G_k E_k(\beta)\right)\right]} \tag{13}$$

where $E_k(\beta)$ are the solutions of Equations (11). If β is too small, the energies $E_k(\beta)$ will be too small also and we will have $\sum_{k=1}^{K} \gamma_k(\beta) > 1$. Increase β until $\sum_{k=1}^{K} \gamma_k(\beta) = 1$ is satisfied.

Let us give the expressions of the allocated energies and sharing factors with respect to the GNRs a_k. Since the random variables $H_k(m, n)$ are circular Gaussian, G_k has the exponential distribution with mean a_k. Let X_e be a positive random variable with the probability density e^{-t}, and let $f(x)$ be the function defined on $[0, \infty)$ as

$$f(x) = \frac{\mathbb{E}\left[\log\left(1 + xX_e\right)\right]}{\mathbb{E}\left[\frac{X_e}{1+xX_e}\right]} - x = \frac{\int \log\left(1 + xt\right) e^{-t} dt}{\int \frac{t}{1+xt} e^{-t} dt} - x = \frac{e^{1/x} x^2 \mathrm{Ei}\left(1/x\right)}{x - e^{1/x} \mathrm{Ei}\left(1/x\right)} - x$$

where Ei is the so-called exponential integral function, defined as $\mathrm{Ei}(x) = \int_x^\infty \frac{e^{-t}}{t} dt$ for $x > 0$.

As G_k is exponentially distributed with mean a_k, it has the same distribution as $a_k X_e$. Therefore, from Equation (12), we have

$$f_k(x) = \frac{1}{a_k} f(a_k x) \ .$$

Powers attribution connected to equations (11) can then be written

$$E_k(\beta) = \frac{1}{a_k} f^{(-1)}(a_k \beta) \tag{14}$$

where $f^{(-1)}$ defined on $[0, \infty)$ is the inverse of f with respect to composition. Thanks to Eq. (14), Eq. (13) can be rewritten as follows

$$\gamma_k(\beta) = \frac{\rho_k}{F(a_k \beta)} \tag{15}$$

where $F(x)$ is the function defined on $\mathbb{R}_+$ by

$$F(x) = \mathbb{E}\left[\log\left(1 + X_e f^{(-1)}(x)\right)\right] .$$

It can be shown that $F(x)$ increases from zero to infinity as x increases from zero to infinity. Moreover, $F(x)$ is continuous on $\mathbb{R}_+^*$.

Since $\sum_{k=1}^{K} \gamma_k(\beta) = 1$, the multiplier β is the unique solution to the following equation

$$\sum_{k=1}^{K} \frac{\rho_k}{F(a_k \beta)} = 1 . \tag{16}$$

It will also be useful to give the expression of Q. It writes

$$Q = \sum_{k=1}^{K} \frac{\rho_k}{a_k} \frac{1}{F(a_k \beta)} f^{(-1)}(a_k \beta) . \tag{17}$$

We obtained an implicit closed-form expression for the minimal energy per channel use that enables us to ensure a rate ρ_k for user k in a single cell environment.

IV. Asymptotic Analysis

The purpose of this section is to give an asymptotic expression of the transmitted energy per channel use (16,17) in the asymptotic regime where the number of users K in the cell grows toward infinity. Our aim is to obtain more tractable expressions that will be useful in particular in the multi-cell situation described in the next section. Assume that user k requires a rate of R_k nats per second. As the number of users grows to infinity, the total required rate $R^{(K)} = \sum_{k=1}^{K} R_k$ grows to infinity. In order to accommodate all the users, we shall assume that the bandwidth B also grows to infinity. The asymptotic regime will therefore be characterized by the fact that $K \to \infty$, $B \to \infty$, and $K/B \to \alpha$ where α is a positive constant. Note that in this regime, the capacities per channel use (*i.e.*, the spectral efficiencies) of the different users $\rho_k = R_k/B$ go to zero.

In order to ensure the convergence of the transmitted energy per channel use in the asymptotic regime and to obtain asymptotic expressions that can be interpreted simply, some additional hypotheses are required.

The cell can be identified with a compact $\mathcal{C}$ included in $\mathbb{R}$ or in $\mathbb{R}^2$ according to whether the cell is one or two dimensional. It is frequent to model the GNR a_k as being directly related to the location x_k of mobile k. Here, x_k is a one or two dimensional variable that represents a point of $\mathcal{C}$ in a coordinate system which origin is occupied by the BS. Getting back to Equation (2), the variance ς_k^2 will be written as $\varsigma_k^2 = q(x_k)$ where $q(x)$ is a continuous function from $\mathcal{C}$ to $\mathbb{R}_+^*$ used to model the so called path loss. With this model, we have $a_k = \pi(x_k)$ where $\pi(x)$ is the GNR profile defined as $\pi(x) = q(x)/N_0$. One widely used example for $q(x)$ is $q(x) = |x|^{-s}$ where $|x|$ denotes the distance between the mobile and the BS, and s is a positive parameter that characterizes the rate of decrease of the signal power with distance. Remember that $q(x)$ is assumed to be defined on $\mathcal{C}$. Therefore, if $q(x) = |x|^{-s}$ is considered, the origin has to be excluded from $\mathcal{C}$. In this situation, it is often assumed that $\mathcal{C} = [-D, -d] \cup [d, D]$ in the one dimensional case, and $\mathcal{C}$ is the closed annulus delimited by circles with radii d and D where d and D are two real numbers such that $0 < d < D$.

The two parameters of user k required to implement the allocation algorithm (14–16) are $\rho_k = R_k/B$ and $a_k = q(x_k)$. By consequence, the user configuration can be equivalently characterized by the set of couples $\{(R_k, x_k)\}_{k=1,\dots,K}$. Describing the set of parameters $\{(R_k, x_k)\}_{k=1,\dots,K}$ is equivalent to providing the following positive measure $\nu^{(K)}$ acting on the Borel sets of $\mathbb{R}_+ \times \mathbb{R}_+$

$$\nu^{(K)}(u,x) = \frac{1}{K}\sum_{k=1}^{K} \delta_{R_k,x_k}(u,x)$$

where δ_{R_k,x_k} is the Dirac measure at the point (R_k, x_k). It is realistic to assume that all required rates belong to an interval $\Delta_R = [R_{\min}, R_{\max}]$ of $\mathbb{R}_+^*$. By consequence, for every $K > 0$, the support of $\nu^{(K)}$ is included in the compact set $\Delta = \Delta_R \times \mathcal{C}$. Notice that $\nu^{(K)}$ is a positive measure satisfying $\int_\Delta d\nu^{(K)} = 1$, and as such, it is a probability measure. Using the fact that $\rho_k = R_k/B$, Equations (16) and (17) can be rewritten respectively as

$$\frac{K}{B}\int_\Delta \frac{u}{F(\pi(x)\beta^{(K)})} d\nu^{(K)}(u,x) = 1 \tag{18}$$

and

$$Q^{(K)} = \frac{K}{B}\int_\Delta \frac{u}{\pi(x)} \frac{f^{(-1)}(\pi(x)\beta^{(K)})}{F(\pi(x)\beta^{(K)})} \, d\nu^{(K)}(u,x) \ . \tag{19}$$

In the last expression, the notation $Q^{(K)}$ is used instead of Q to put ahead the fact that we now have a sequence of energies per channel use indexed by the number of users. The multiplier β is denoted $\beta^{(K)}$ similarly. Convergence of this sequence will come from the following assumption:

(B1) As $K \to \infty$, the sequence of measures $\nu^{(K)}$ converges weakly to a probability measure ν.

It is realistic to assume that the limit joint distribution ν of rates and users locations is the measure product of a limit rate distribution times a limit location distribution. This is justified heuristically by a notion of independence between the rate requirements of the users and their locations:

(B2) The measure ν satisfies $d\nu(u,x) = d\zeta(u) \times d\lambda(x)$ where ζ is the limit distribution of rates and λ is the limit distribution of the user locations x_k. Both ζ and λ are probability measures. Here $\times$ denotes the product of measures.

Typically, the measure λ can be modeled as the uniform probability measure over $\mathcal{C}$, in other words $d\lambda(x) = (1/|\mathcal{C}|)\, dx$ where $|\mathcal{C}|$ is the cell volume. Concerning the limit rate distribution ζ, denote by $\overline{R} = \int_{\Delta_R} u d\zeta(u)$ its mean. A parameter that will be of prime importance in the following is the mean rate $\overline{r}$ per channel use and per cell volume unit. It is given by $\overline{r} = \alpha \overline{R}/|\mathcal{C}|$ nats per channel use and per (squared) meter.

We turn now to the asymptotic expressions. We have the following theorem:

Theorem 1: Assume $K \to \infty$ in such a way that $K/B \to \alpha > 0$, and that the measure $\nu^{(K)}$ satisfies assumptions (B1) and (B2). Assume that $\pi(x)$ is continuous and satisfies $\pi(x) > 0$ on $\mathcal{C}$. Then $Q^{(K)}$ converges to Q given by

$$Q = \overline{r} \int_{\mathcal{C}} \frac{f^{(-1)}(\pi(x)\beta)}{\pi(x)\ F\left(\pi(x)\beta\right)}\ |\mathcal{C}| d\lambda(x) \tag{20}$$

where β is the unique positive number that satisfies

$$\overline{r} \int_{\mathcal{C}} \frac{|\mathcal{C}|}{F\left(\pi(x)\beta\right)} d\lambda(x) = 1. \tag{21}$$

This theorem which proof is in Appendix A is the main result of the paper in the single cell environment. One interesting consequence of Theorem 1 is that the rate distribution affects the asymptotic energy per channel use through its mean only. On other words, in the asymptotic regime, the minimal power consumed for achieving the individual user rates depends only on the global rate requirement. It does not depend on the particular form of the individual rate distribution.

V. The Multi-Cell Environment

In GSM mobile cellular system, the spectrum is split into several sub-bands, and adjacent cells do not share the same sub-band. Consequently there is no multi-cell interference coming from adjacent cells. But such a system requires a frequency planning and prevents soft handover. Therefore advanced cellular systems (e.g., UMTS) will work with an universal frequency re-use to take benefit of the soft handover, of the macro-diversity, and of a flexible frequential management. To carry out an universal frequency re-use system, any spread-spectrum based multiple acces technique, such as DS-CDMA or FH-OFDMA, can be employed [13].

Consequently, in this section, we modify and analyze the behavior of the power allocation algorithm in a multi-cell environment, *i.e.* when, in addition to the background noise, the signal received by a user is corrupted by the signals sent by the Base Stations of other cells. We prove that the power allocation strategy is quite different from the single cell case and especially there exists a maximum value for the rate. Beyond this threshold, the multi-cell interference strongly disturbs the transmission and does not enable us to get reliable transmission.

A. Cell Model

We consider for simplicity a one dimensional cellular system that consists of a linear regular array of cells as shown in figure 2. In this figure, D is the half distance between two neighboring BS, and a cell is included in the interval $[-D, D]$ if we identify its BS with the origin. Even if such a multi-cell model, studied in [14] and [15] is an ideal model, it provides some interesting guidelines that help to implement a practical cellular system. Here, to simplify our presentation, we furthermore assume that the Multi-Cell Interference (MCI) comes from the adjacent cells only; we thus neglect the MCI due to further cells. Suppose that, at OFDM symbol m, the signal sent by the BS on sub-carrier n is

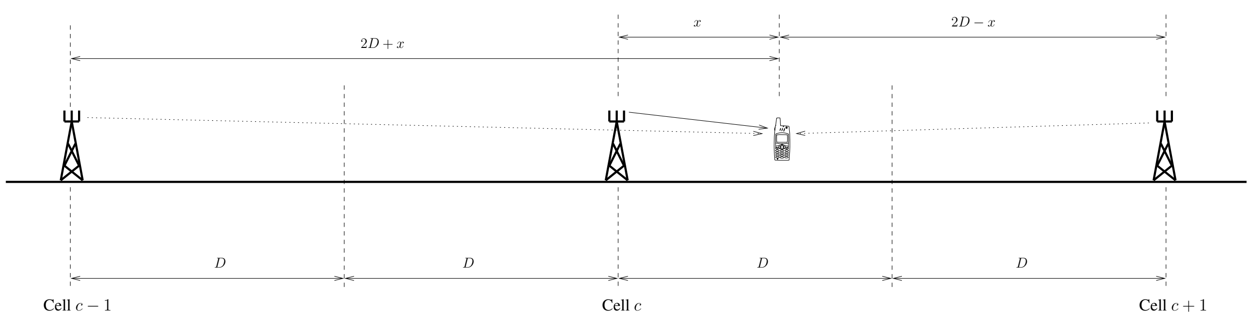

Fig. 2. The multi-cell environment

intended to user k. In a single cell environment, the received signal $Y_k(m,n)$ is then written $Y_k(m,n) = H_k(m,n)S(m,n) + V_k(m,n)$ as shown in Equation (1). To give the expression of the received signal in a multi-cell environment, let us number the cells as indicated in the figure and put the superscript $^{(c)}$ to refer to the quantities located to cell number c. For instance the signal transmitted by BS number c will be denoted $S^{(c)}(m,n)$. Consistently with the notations of section II, we denote by $\mathbf{h}_k^{(c',c)}(m)$ the impulse response of the channel that carries the signal of BS number c' to user k of cell c, and by $\mathbf{H}_k^{(c',c)}(m)$ its Discrete Fourier Transform. With these notations, the signal received by user k of cell c at OFDM symbol m and sub-carrier n becomes

$$Y_k^{(c)}(m,n) = H_k^{(c)}(m,n)S^{(c)}(m,n)+H_k^{(c-1,c)}(m,n)S^{(c-1)}(m,n)+H_k^{(c+1,c)}(m,n)S^{(c+1)}(m,n)+V_k^{(c)}(m,n)\,. \tag{22}$$

We assume that a frequency hopping algorithm is implemented in all cells and that this algorithm ensures that the signal of any user is equally distributed on all sub-carriers. It results from this assumption that $\mathbb{E}\left[\left|S^{(c)}(m,n)\right|^2\right] = BQ^{(c)}$ for all m and n. If we furthermore suppose that the inter-cell channels $\mathbf{h}_k^{(c',c)}(m)$ satisfy assumption (A), then the variance of $H_k^{(c-1,c)}(m,n)$ is independent of m and n as in section II. In this case, the GNR $a_k^{(c)}$ of user k in cell c is written

$$a_k^{(c)} = \frac{\mathbb{E}\left[\left|H_k^{(c)}(m,n)\right|^2\right]}{Q^{(c-1)}\mathbb{E}\left[\left|H_k^{(c-1,c)}(m,n)\right|^2\right] + Q^{(c+1)}\mathbb{E}\left[\left|H_k^{(c+1,c)}(m,n)\right|^2\right] + N_0}\,.$$

Let us consider the problem of the capacity derivation. The noise $V_k(m,n)$ in Equation (1) is replaced in the multi-cell case by the noise $\tilde{V}_k(m,n) = H_k^{(c-1,c)}(m,n)S^{(c-1)}(m,n) + H_k^{(c+1,c)}(m,n)S^{(c+1)}(m,n) + V_k^{(c)}(m,n)$ as shown in Equation (22). As this noise is clearly non-Gaussian, the capacity is in general difficult to derive. Nevertheless, if we endow $S^{(c)}(m,n)$ with the Gaussian distribution, then the associated mutual information between $S^{(c)}(m,n)$ and $Y_k^{(c)}(m,n)$ is a lower bound to the capacity. It is furthermore well known that when the variances of the information signal and the noise are fixed and the information signal is Gaussian, then the mutual information is minimum when the noise is Gaussian [16]. Therefore we can easily derive a lower bound on the true capacity if we approximate the multi-cell interference noise by a Gaussian noise with the same variance. Then we are essentially led back to the situation of section II.

As we shall require this lower bound to satisfy the rate constraints, the obtained power will represent an upper bound on the power necessary in theory to comply with these constraints.

In short, energies per channel use and shares are still computed according to Equations (14–16) with the difference that a_k is replaced by $a_k^{(c)}$. Note that the quantities $a_k^{(c)}$ can be consistently estimated by the BS number c.

Let us now consider the asymptotic regime in the multi-cell situation. In order to apply a path-loss model to the inter-cell channels, we extend the set of definition of the function $q(x)$ to $\mathcal{C} \cup (2D + \mathcal{C}) \cup (2D - \mathcal{C})$ where $2D \pm \mathcal{C} = \{2D \pm x,\ x \in \mathcal{C}\}$, and assume that $q(x)$ is continuous on this domain. With this extension, we have $\mathbb{E}\left[\left|H_k^{(c-1,c)}(m,n)\right|^2\right] = q(2D+x)$ and $\mathbb{E}\left[\left|H_k^{(c+1,c)}(m,n)\right|^2\right] = q(2D-x)$ (see figure 2). Let us denote by $\pi_{Q^{(c-1)},Q^{(c+1)}}(x)$ the GNR profile in the conditions described by Equation (22). This function is written

$$\pi_{Q^{(c-1)},Q^{(c+1)}}(x) = \frac{q(x)}{Q^{(c-1)}q(2D+x) + Q^{(c+1)}q(2D-x) + N_0} \ .$$

In a multi-cell setting, a lower bound on the total energy per channel use is therefore given by Equation (20) where β satisfies (21), and in both equations, $\pi(x)$ is replaced by $\pi_{Q^{(c-1)},Q^{(c+1)}}(x)$.

B. The Equilibrium Energy per Channel Use

Any BS combats the MCI coming from its neighbors by increasing its own transmitted power. By doing so, it will however increase the interference it produces with its neighboring cells, so that these cells will have to increase in turn their powers, and so forth. In this section, we tackle the problem of finding a condition under which the whole cell array can nevertheless reach an equilibrium. Here we consider an infinite array and we assume that each cell satisfies the conditions of the asymptotic regime. To simplify our analysis, we assume that at a certain moment that we call moment zero, all cells transmit at power $Q_0 B$. For instance, one can imagine that moment zero is the moment where all BS are "switched on" simultaneously, in which case one would have $Q_0 = 0$. After executing the allocation algorithm, each BS will transmit a signal with the energy per channel use given by Equation (20) that we denote here Q_1. At a later moment called moment one, the cells will execute again the algorithm simultaneously then deliver the energy Q_2. By iterating, the energy Q_{n+1} delivered by each BS at moment n will be given by the following expressions. Let $\beta(Q,\overline{r})$ be the unique solution to the equation (see Eqs (18) and (19))

$$\overline{r}\int_{\mathcal{C}} \frac{|\mathcal{C}|}{F\left(\underline{\pi}_Q(x)\beta(Q,\overline{r})\right)} d\lambda(x) = 1 \tag{23}$$

where $\underline{\pi}_Q(x)$ is given by

$$\underline{\pi}_Q(x) = \pi_{Q,Q}(x) = \frac{q(x)}{Q\left(q(2D+x)+q(2D-x)\right)+N_0} \ , \tag{24}$$

and define $\xi(Q,\overline{r})$ as

$$\xi(Q,\overline{r}) = \overline{r}\int_{\mathcal{C}} \frac{f^{(-1)}\left(\underline{\pi}_Q(x)\beta(Q,\overline{r})\right)}{\pi_Q(x)\ F\left(\underline{\pi}_Q(x)\beta(Q,\overline{r})\right)}\ |\mathcal{C}| d\lambda(x) \ . \tag{25}$$

$\xi(Q,\overline{r})$ is the total energy per channel use a cell needs to transmit to attain the mean rate of $\overline{r}$ nats per channel use and cell volume unit when its neighboring cells transmit at energy Q. The energy Q_{n+1} will be given by

$$Q_{n+1} = \xi(Q_n,\overline{r}) \ . \tag{26}$$

The convergence of this sequence is treated by the following theorem which is the main result of this section:

Theorem 2: Let $t(x)$ be defined on $\mathcal{C}$ as

$$t(x) = \frac{q(x)}{q(2D-x)+q(2D+x)} \ .$$

Assume that $t(x)$ is continuous and satisfies $t(x) > 0$ on $\mathcal{C}$. Define $\psi(r)$ on $\mathbb{R}_+^*$ as

$$\psi(r) = r \int_{\mathcal{C}} \frac{f^{(-1)}(t(x)b(r))}{t(x)F\left(t(x)b(r)\right)} \ |\mathcal{C}| d\lambda(x) \tag{27}$$

where $b(r)$ is the unique positive number that satisfies

$$r \int_{\mathcal{C}} \frac{|\mathcal{C}|}{F(t(x)b(r))} \ d\lambda(x) = 1 \ . \tag{28}$$

Then

1) the equation $\psi(r) = 1$ admits an unique solution $r_0 > 0$.
2) for any initial value $Q_0 \geq 0$, if $\overline{r} < r_0$, then the sequence (Q_n) which elements are given by (26) converges, and if $\overline{r} \geq r_0$, then it grows to infinity.

This theorem can be proven thanks to the following three lemmas:

Lemma 1: For every $r > 0$, the function $\xi(Q, r)$ defined in (25) satisfies the following properties: $\xi(0, r) > 0$, $\xi(Q, r)$ is increasing in the variable Q on $\mathbb{R}_+$, and $\xi(Q, r)/Q$ is decreasing in Q on $\mathbb{R}_+^*$.

Lemma 2: $\lim_{Q \to \infty} \xi(Q, r)/Q = \psi(r)$ where ψ is given by (27).

Lemma 3: $\lim_{r \to 0} \psi(r) = 0$ and $\lim_{r \to \infty} \psi(r) = \infty$. Furthermore $r \mapsto \psi(r)$ is increasing.

These lemmas are respectively proven in Appendices B, C, and D. Finally the proof of Theorem 1 is drawn in Appendix E.

Practically this theorem indicates that

- If the rate is less than a certain threshold r_0, then the multi-cell system can operate ;
- For a given achievable rate, *i.e*, a rate less than the threshold r_0, the proposed allocation strategy converges and minimizes the power consumption. Notice that this part of the theorem is similar to the single cell case.

VI. NUMERICAL ILLUSTRATIONS

We begin by introducing the channel models that we considered. Simulations are carried out using three different path loss exponent values: $s = 2, 3$ and 3.5 as introduced in section IV. We consider a Free Space Loss (FSL) model characterized by a path loss exponent $s = 2$, and the so-called Okumura-Hata

(O-H) model for open areas, which is widely used for predicting path loss in mobile wireless systems ([17]). For the O-H case, we consider the cases $s = 3$ and $s = 3.5$.

The carrier frequency is $f_0 = 1.8$ GHz. At this frequency, the basic equations for path loss in dB are :

$$\begin{array}{lll} \text{FSL} & : & \pi^{\text{I}}_{\text{dB}}(x_{\text{km}}) = 20\log_{10}(x_{\text{km}}) + 97.5 \\ \text{O-H} \quad s = 3 & : & \pi^{\text{II}}_{\text{dB}}(x_{\text{km}}) = 30\log_{10}(x_{\text{km}}) + 93.3 \\ \text{O-H} \quad s = 3.5 & : & \pi^{\text{III}}_{\text{dB}}(x_{\text{km}}) = 35\log_{10}(x_{\text{km}}) + 103.8 \end{array}$$

where x_{km} is the distance in km between the BS and the receiver. The default values for the cell inner radius d and outer radius D are set to 150 m and 5 km respectively. Finally, the signal bandwidth is $B = 5\text{MHz}$ and the noise Power Spectral Density is $N_0 = -170$ dBm/Hz.

We first validate the asymptotic analysis in a single cell context with the FSL model. We consider a mean rate request $\overline{r}$ of 0.5 bit per second per channel use and per kilometer and compare the power QB required by our allocation algorithm (cf. (17)) for a number of users K varying between 5 and 100, and the power $Q^{(K)}B$ required in asymptotic regime (cf. (20)). On Figure 3, we plotted the normalized MSE, *i.e.*, $(Q - Q^{(K)})^2/(Q^{(K)})^2$.

On Figures 4 and 5, we also compute the power required by the BS to reach a mean rate $\overline{r}$ of 0.2 and 0.5 bit per second, per channel use and per kilometer, versus the cell radius for various channel models in the single cell context. We use the asymptotic approximations provided by Equations (20) and (21). We assume that the transmitted power is limited to 20 W, which corresponds to the upper border of the figures.

These curves give useful guidelines for cell dimensioning : given a constraint on the transmitted power, we directly deduce the corresponding size of the cell that can be covered by the BS. For instance, if the maximal transmitted power is 1 W, the cell radius can not be greater than 14 km for a mean rate requirement of 0.2 bit/s/Hz/km under the FSL model. In the same conditions, the maximal radius becomes 7.5 km for a mean rate value of 0.5 bit/s/Hz/km.

In a multi-cell environment, the BS coverage performance is seriously degraded by multi-cell interference. In Figure 6, the mean required rate is set to $\overline{r} = 0.2$ bit/s/Hz/km like for Fig. 4. Fig. 6 shows that the maximal cell radius is reduced from 14 km to 5.4 km. Moreover, on Figure 7, the maximal cell radius is shrinks from 7.5 km (see Fig. 5) to 2.2 km for a mean rate requirement of 0.5 bit/s/Hz/km. Furthermore it is worth noticing a major difference between single-cell and multi-cell contexts : the curves obtained in the multi-cell context grow to infinity when the cell radius D reaches a certain threshold. This value depends on s and on $\bar{r}$. For instance, in the free space model, for a mean rate requirement of

0.2 bits/s/Hz/m, a limit is located at $D = 5.4$ km.

To justify the existence of these limits, let us now focus on how the multi-cell results were obtained. Figure 8 represents the function denoted $\xi(Q, \bar{r})$ given by (25) for three different values of $\bar{r}$. For each value of Q, we first find $\beta(Q, \bar{r})$ defined as the unique solution of Equation (23), and then we compute $\xi(Q, \bar{r})$. The equilibrium power is given by the fixed point coordinates which can be determined geometrically by the intersection of $\xi(Q, \bar{r})$ with the first bisector, shown as a solid line on the figure 8. The values of Q corresponding to the different mean rate requirements are gathered in Table I. Q naturally increases with $\bar{r}$, and so does $\psi(\bar{r})$. Therefore, as predicted by Theorem 2, there exists a limit on the mean rate demand r_0 beyond which $\xi(Q, \bar{r})$ and the first bisector do not meet. Figure 9 represents r_0 versus the cell radius in km for the three path loss models. For a given cell radius D, any mean rate lower than r_0 can be satisfied *i.e.*, the algorithm converges for any $\bar{r} < r_0$. Symmetrically, to any mean rate $\bar{r}$, corresponds a maximal coverage radius D. As a consequence, for a given $\bar{r}$, when D tends to the corresponding limit radius, Q tends to infinity, which explains the presence of the asymptotes on Figures 6 and 7.

$\bar{r}$ (bit/s/Hz/km)	QB (W)
0.15	1.08×10^{-2}
0.2	8.55×10^{-2}
0.21	0.95

TABLE I

EQUILIBRIUM POWER (INTERSECTION POINTS ON FIGURE 8)

Our FH-OFDMA allocation strategy is based on an universal frequency re-use (i.e., a frequency re-use factor of one). It would be interesting to compare this allocation strategy to a strategy that assigns different frequency bands to adjacent cells, which amounts to a frequency re-use factor of one half for one dimensional cells. With a frequency re-use factor of one, more (macro and frequency) diversity can be collected and the technical constraints due to frequency planning are avoided. In contrast, compared to the strategy with frequency planning, the signal to noise ratio per sub-carrier degrades because of the MCI. In Figure 10, we compare both strategies by plotting the consumed power versus the size of the cell for a given mean required rate per cell volume. In the case of FH-OFDMA with a re-use factor of one, we consider the mean rate $\bar{r} = 0.2$bit/s/Hz/km and the power QB where $B = 5\text{MHz}$ is the total

bandwidth used by the system. In order to ensure the same mean rate requirement per cell volume, the approach with frequency planning is carried out by simply turning back to the single cell case (introduced in Section II) and by considering the mean rate requirement $\overline{r}' = 0.4$bit/s/Hz/km and a power equal to $Q'B/2$ where Q' is obtained via Eq. (16) and (17).
We notice that the required power per BS without frequency planning is slightly smaller than the power with frequency planning as long as the cell radius is smaller than a given threshold that depends on the path loss exponent s. Beyond this threshold, frequency planning is better from the point of vue of total consumed power. This threshold is equal to 3.2km, 5.6km, and 6.7km for $s = 2, 3$, and 3.5 respectively. For reasonable values of cell radius, it is useless to implement frequency planning.

APPENDIX

A. Proof of Theorem 1

Because $F(x)$ increases from zero to infinity on $\mathbb{R}_+$, it is clear that β is the unique solution of Equation (21). We shall show that $\beta^{(K)}$ given by (18) converges to β. Equation (21) can be rewritten as

$$\alpha \int_\Delta \frac{u}{F(\pi(x)\beta)} d\nu(u,x) = 1 \ . \tag{29}$$

The function $F(x)$ is continuous and strictly positive on any compact subset of $\mathbb{R}_+^*$. Due to the assumptions on $\pi(x)$, the function $F(\pi(x)\beta)$ is continuous and satisfies $F(\pi(x)\beta) > 0$ on the compact set Δ for every $\beta > 0$. Therefore, for any $\beta > 0$, $u/F(\pi(x)\beta)$ is continuous on Δ. By applying standard results related to the convergence of measures [18], and by using (29), we therefore have

$$\frac{K}{B} \int_\Delta \frac{u}{F(\pi(x)\beta)} d\nu^{(K)}(u,x) \to 1 \ . \tag{30}$$

Let $\pi_{\min} = \min_{x\in\mathcal{C}} \pi(x)$ and $\pi_{\max} = \max_{x\in\mathcal{C}} \pi(x)$. By assumption, we have $\pi_{\min} > 0$. From (18), we have the inequality

$$\frac{K}{B}\frac{R_{\min}}{F\left(\beta^{(K)}\pi_{\max}\right)} \le 1 \le \frac{K}{B}\frac{R_{\max}}{F\left(\beta^{(K)}\pi_{\min}\right)}$$

Using the fact that $F(x)$ is increasing from zero to infinity, these inequalities show that for K large enough, all $\beta^{(K)}$ belong to a compact set $[\beta_{\min}, \beta_{\max}]$ with $\beta_{\min} > 0$. By applying the same argument to (29), we show that $\beta \in [\beta_{\min}, \beta_{\max}]$ also. Thanks to equation (18), the convergence stated in (30) can be rewritten

$$\frac{K}{B} \int_\Delta \left(\frac{1}{F(\pi(x)\beta)} - \frac{1}{F(\pi(x)\beta^{(K)})} \right) \ u \ d\nu^{(K)}(u,x) \to 0 \ . \tag{31}$$

Assume that $|\beta^{(K)} - \beta| > \eta$ for some $\eta > 0$. Then $\left|\pi(x)\beta^{(K)} - \pi(x)\beta\right| > \eta\pi_{\min}$ for all $x \in \mathcal{C}$. The function $F(x)$ is continuous on the compact interval $[\beta_{\min}\pi_{\min}, \beta_{\max}\pi_{\max}]$, therefore it is uniformly continuous on this interval, hence $\left|F(\pi(x)\beta) - F(\pi(x)\beta^{(K)})\right|$ is larger than a certain $\epsilon > 0$ for all $x \in \mathcal{C}$. We shall therefore have

$$\begin{aligned}\frac{K}{B}\left|\int_\Delta \left(\frac{1}{F(\pi(x)\beta)} - \frac{1}{F(\pi(x)\beta^{(K)})}\right) u \, d\nu^{(K)}(u,x)\right| &= \frac{K}{B}\int_\Delta \frac{\left|F(\pi(x)\beta^{(K)}) - F(\pi(x)\beta)\right|}{F(\pi(x)\beta)F(\pi(x)\beta^{(K)})} u \, d\nu^{(K)}(u,x) \\ &\geq \frac{K}{B}\frac{\epsilon}{F\left(\beta_{\max}\pi_{\max}\right)^2}\int_\Delta u \, d\nu^{(K)}(u,x) \\ &\geq \frac{K}{B}\frac{\epsilon}{F\left(\beta_{\max}\pi_{\max}\right)^2} R_{\min}\end{aligned}$$

which contradicts (31). Therefore, $\beta^{(K)} \to \beta$. With this, one can establish without difficulty the convergence of $Q^{(K)}$ toward Q by considering equations (19) and (20). ■

B. Proof of Lemma 1

The first assertion can be established by noticing that $\xi(0,r)$ is the energy per channel use needed in the single cell case to ensure a mean rate per channel use and cell volume unit equal to r.

To prove the second assertion, let us get back to the non-asymptotic regime and denote by $\mathbf{r}^{(K)} = [R_1, \ldots, R_K]$ a certain vector of K rates, and by $\mathbf{x}^{(K)} = [x_1, \ldots, x_K]$ a vector of K mobile locations. If the cell undergoes from its neighbors a MCI with power QB, then the GNRs of the K mobiles is given by $\underline{\pi}_Q(x_k)$. The total energy per channel use that the BS transmit after computing the allocation algorithm in these conditions is denoted by $\xi^{(K)}(\mathbf{r}^{(K)}, \mathbf{x}^{(K)}, Q)$. Associate with the vectors $\mathbf{r}^{(K)}$ and $\mathbf{x}^{(K)}$ the measure $\nu^{(K)} = \frac{1}{K}\sum_{k=1}^K \delta_{R_k,x_k}$, and assume that $\nu^{(K)}$ satisfies assumption (B1). Then $\xi^{(K)}(\mathbf{r}^{(K)}, \mathbf{x}^{(K)}, Q) \to \xi(Q,r)$ as $K \to \infty$ thanks to Theorem 1. Therefore, if we prove that $\xi^{(K)}(\mathbf{r}^{(K)}, \mathbf{x}^{(K)}, Q)$ is increasing in the parameter Q for all K, the second assertion will be proven thanks to the limit operator.

Let $g(x)$ be the function defined on $\mathbb{R}_+$ as $g(x) = \mathbb{E}\left[\log(1 + X_e x)\right]$ where X_e is a random variable with the exponential distribution with mean one. According to Eq. (7), the rate of user k is provided by $R_k = B\gamma_k g\left(Q_k \underline{\pi}_Q(x_k)/\gamma_k\right)$ with the share γ_k and the energy per channel use Q_k. Denote by $g^{(-1)}(x)$ the inverse on $\mathbb{R}_+$ of $g(x)$ with respect to composition. Then the energy $\xi^{(K)}(\mathbf{r}^{(K)}, \mathbf{x}^{(K)}, Q)$ is the minimum of the function

$$\Xi^{(K)}(\boldsymbol{\gamma}^{(K)}, \mathbf{r}^{(K)}, \mathbf{x}^{(K)}, Q) = \sum_{k=1}^K Q_k = \sum_{k=1}^K \frac{\gamma_k}{\underline{\pi}_Q(x_k)} g^{(-1)}\left(\frac{R_k}{\gamma_k B}\right)$$

with respect to the vector $\boldsymbol{\gamma}^{(K)} = [\gamma_1, \ldots, \gamma_K]^{\mathrm{T}}$ over the unit simplex $\mathcal{S} = \{\boldsymbol{\gamma}^{(K)} : \gamma_1 \geq 0, \ldots, \gamma_K \geq 0, \sum_{k=1}^K \gamma_k \leq 1\}$. If $Q_1 \geq Q_2$, then $\underline{\pi}_{Q_1}(x_k) \leq \underline{\pi}_{Q_2}(x_k)$ for all k, and therefore $\Xi^{(K)}(\boldsymbol{\gamma}^{(K)}, \mathbf{r}^{(K)}, \mathbf{x}^{(K)}, Q_1) \geq \Xi^{(K)}(\boldsymbol{\gamma}^{(K)}, \mathbf{r}^{(K)}, \mathbf{x}^{(K)}, Q_2)$ for every $\boldsymbol{\gamma}^{(K)} \in \mathcal{S}$. Recall that if two real functions f_1 and f_2 satisfy $f_1(x) \geq f_2(x)$ on some set S, then $\min_{x\in S} f_1(x) \geq \min_{x\in S} f_2(x)$. This implies that $\xi^{(K)}(\mathbf{r}^{(K)}, \mathbf{x}^{(K)}, Q_1) \geq$

$\xi^{(K)}(\mathbf{r}^{(K)}, \mathbf{x}^{(K)}, Q_2)$, which proves the second assertion.

To prove the third assertion, we notice that

$$\frac{\Xi^{(K)}(\boldsymbol{\gamma}^{(K)}, \mathbf{r}^{(K)}, \mathbf{x}^{(K)}, Q)}{Q} = \sum_{k=1}^{K} \gamma_k \frac{q(2D+x_k) + q(2D-x_k) + \frac{\sigma^2}{Q}}{q(x_k)} g^{(-1)}\left(\frac{R_k}{\gamma_k B}\right)$$

over $\mathcal{S}$. It is clear that for $Q_1 \geq Q_2$, $\Xi^{(K)}(\boldsymbol{\gamma}^{(K)}, \mathbf{r}^{(K)}, \mathbf{x}^{(K)}, Q_1)/Q_1 \leq \Xi^{(K)}(\boldsymbol{\gamma}^{(K)}, \mathbf{r}^{(K)}, \mathbf{x}^{(K)}, Q_2)/Q_2$. The result follows from the same argument as above. ■

C. Proof of Lemma 2

Equation (25) can now be rewritten as

$$\frac{\xi(Q,r)}{Q} = r \int_{\mathcal{C}} \frac{f^{(-1)}\left(\frac{\beta(Q,r)}{Q} z(Q,x)\right)}{z(Q,x)\ F\left(\frac{\beta(Q,r)}{Q} z(Q,x)\right)} |\mathcal{C}| d\lambda(x) \tag{32}$$

where

$$z(Q,x) = \frac{q(x)}{q(2D-x) + q(2D+x) + N_0/Q}$$

and where $\beta(Q,r)$ is the solution of (23).

It is obvious that $z(Q,x) - t(x) \to 0$ as $Q \to \infty$. Moreover for any $A > 0$, due to the non-nullity and the continuity of $q(x)$ on the compact $\mathcal{C}$, one can check that $z(Q,x) > C_A$ with $C_A > 0$, whatever $Q > A$.

Now we shall prove that $\beta(Q,r)/Q$ is bounded. Indeed, as $z(Q,x) < t(x)$, we have

$$1 = r \int_{\mathcal{C}} \frac{|\mathcal{C}|}{F\left(\frac{\beta(Q,r)}{Q} z(Q,x)\right)}\ d\lambda(x)\ > r \int_{\mathcal{C}} \frac{|\mathcal{C}|}{F\left(\frac{\beta(Q,r)}{Q} t(x)\right)}\ d\lambda(x)\ \geq r \frac{|\mathcal{C}|}{F\left(\frac{\beta(Q,r)}{Q} t_{\max}\right)}$$

where $t_{\max} = \max_{x\in\mathcal{C}} t(x)$. Since $F(.)$ is increasing from zero to infinity, previous inequalities show that $\beta(Q,r)/Q$ is lower-bounded. Furthermore, by using the lower bound of $z(Q,x)$, we obtain that

$$1 = r \int_{\mathcal{C}} \frac{|\mathcal{C}|}{F\left(\frac{\beta(Q,r)}{Q} z(Q,x)\right)}\ d\lambda(x) < r \frac{|\mathcal{C}|}{F\left(\frac{\beta(Q,r)}{Q} C_A\right)}\ .$$

For the same reasons as above, $\beta(Q,r)/Q$ is upper-bounded. Consequently

$$\frac{\beta(Q,r)}{Q} z(Q,x) - \frac{\beta(Q,r)}{Q} t(x) \xrightarrow[Q\to\infty]{} 0 \tag{33}$$

As $x \mapsto (\beta(Q,r)/Q) z(Q,x)$ is strictly positive and continuous on the compact $\mathcal{C}$, and as $F(.)$ is also strictly positive and continuous on $\mathbb{R}^+$, we get $x \mapsto F((\beta(Q,r)/Q) z(Q,x))$ is strictly positive and continuous on the compact $\mathcal{C}$. Therefore we obtain

$$r \int_{\mathcal{C}} \frac{|\mathcal{C}|}{F\left(\frac{\beta(Q,r)}{Q} t(x)\right)}\ d\lambda(x) \xrightarrow[Q\to\infty]{} 1. \tag{34}$$

Consequently due to the continuity of $F(.)$ and the unicity of the solution of (23), we have that $\beta(Q,r)/Q$ converges toward $b(r)$ as $Q \to \infty$. Plugging in Eq. (32), we obtain the result. ■

D. Proof of Lemma 3

We begin by showing that $b(r)$ increases from zero to infinity on $\mathbb{R}_+$. It is clear by inspecting (28) that $b(r)$ is an increasing function. Let us show that $b(r) \to 0$ as $r \to 0$. Assume $b(r) > \eta$ for a given $\eta > 0$. Then $F\left(b(r)t(x)\right) > F\left(\eta \min_{x\in\mathcal{C}}(t(x))\right)$ on $\mathcal{C}$, and therefore,

$$\int_{\mathcal{C}} \frac{|\mathcal{C}|}{F\left(b(r)t(x)\right)}\, d\lambda(x) < \frac{|\mathcal{C}|}{F\left(\eta \min_{x\in\mathcal{C}}(t(x))\right)}$$

From (28), we then have, $b(r) > \eta \Rightarrow r > C$ with $C = F\left(\eta \min_{x\in\mathcal{C}}(t(x))\right)/|\mathcal{C}| > 0$. This implies that $b(r) \to 0$ as $r \to 0$. One can show similarly that $b(r) \to \infty$ as $r \to \infty$.

The function $\psi(r)$ can be decomposed as follows :

$$\psi(r) = |\mathcal{C}| r \int_{\mathcal{C}} \frac{\phi(g(r,x))}{t(x)} d\lambda(x) \tag{35}$$

where

$$\phi(\rho) = \frac{\rho}{\mathbb{E}_{X_e}[\log(1+X_e\rho)]} = \frac{\rho}{e^{1/\rho}\mathrm{Ei}(1/\rho)}$$

and

$$g(r,x) = f^{(-1)}(t(x)b(r)).$$

It is easy to check that $\rho \mapsto \phi(\rho)$ and $r \mapsto g(r,x)$ for each fixed x are increasing functions. According to Eq. (35), we deduce that ψ is increasing.

■

E. Proof of Theorem 2

From lemmas 1 and 2, $\xi(Q,r)/Q$ decreases from infinity to $\psi(r)$, and by lemma 3, $\psi(r) < 1$ if and only if $r < r_0$. Consequently the equation $\xi(Q,r) = Q$ admits a solution (which is unique) denoted by Q_s if and only if $r < r_0$. In such a case, the sequence (Q_n) converges to Q_s whatever the initial value Q_0. Indeed, if $Q_0 < Q_s$, then the sequence (Q_n) is increasing and bounded : as $\xi(Q,r) > Q$ for $Q < Q_s$, we have $Q_1 = \xi(Q_0,r) \geq Q_0$. Assume that $Q_n \geq Q_{n-1}$. Because $\xi(Q,r)$ is increasing in Q as stated in lemma 1, we have $Q_{n+1} = \xi(Q_n,r) \geq \xi(Q_{n-1},r) = Q_n$. Therefore, (Q_n) is increasing. As $Q_0 < Q_s$ and $\xi(Q,r)$ is increasing, $Q_1 = \xi(Q_0,r) \leq \xi(Q_s,r) = Q_s$, and by the same argument, $Q_n \leq Q_s$ for every n. Therefore (Q_n) is increasing and bounded and thus converges. Since $Q \mapsto \xi(Q,r)$ is continuous and Q_s is the unique solution of $\xi(Q,r) = Q$, the sequence (Q_n) converges toward Q_s.

By a similar argument, one shows that if $Q_0 > Q_s$, then the sequence (Q_n) decreases toward Q_s.
It remains to prove that if $r \geq r_0$, then (Q_n) diverges. Here, we have $\xi(Q,r) > Q$ for any value of Q. Therefore, the sequence (Q_n) is increasing. Let us show that it is unbounded. Assume the contrary, in other words there exists $\overline{Q} > 0$ such that $Q_n < \overline{Q}$ for every n. Let $e = \xi(\overline{Q},r)/\overline{Q} - 1$. Because $r \geq r_0$, we have $e > 0$. As $\xi(Q,r)/Q$ is decreasing, we have $\xi(Q,r)/Q - 1 \geq e$ for every $Q < \overline{Q}$. By consequence, the elements of (Q_n) satisfy $Q_{n+1} - Q_n \geq Q_n e \geq Q_1 e$ for every n. Therefore, for $n \geq \frac{\overline{Q}}{Q_1 e}$, we have $Q_n > \overline{Q}$ which is a contradiction. ■

References

[1] K. Stamatiou and J. Proakis, "A performance analysis of coded Frequency-Hopped OFDMA," in *Proceedings of the IEEE Wireless Communications and Networking Conference*, 2005, pp. 1132–1137.

[2] R. Laroia, S. Uppala, and J. Li, "Designing a Mobile Broadband Wireless Access Network," *IEEE Signal Processing Magazine*, pp. 20–28, Sept. 2004.

[3] C.Y. Wong, R.S. Cheng, K. Ben Letaief, and R.D. Murch, "Multiuser OFDM with Adaptive Subcarrier, Bit and Power Allocation," *IEEE Journal on Selected Areas in Communications*, vol. 17, no. 10, pp. 1747–1758, Oct. 1999.

[4] D. Kivanc and H. Liu, "Subcarrier Allocation and Power Control for OFDMA," in *Proc. of the 34th Asilomar Conference on Signals, Systems and Computers*, 2000, pp. 147–151.

[5] S. Pietrzyk and G.J.M Janssen, "Multiuser subcarrier allocation for QoS provision in the OFDMA systems," in *Proceedings of the IEEE Vehicular Technology Conference*, 2002, pp. 1077–1081.

[6] M. Ergen, S. Coleri, and P. Varaiya, "QoS aware adaptive resource allocation techniques for fair scheduling in OFDMA based broadband wireless access systems," *IEEE Trans. on Broadcasting*, vol. 49, no. 4, pp. 362–370, Dec. 2003.

[7] D. Kivanc, G. Li, and H. Liu, "Computationally efficient bandwidth allocation and power control for OFDMA," *IEEE Trans. on Wireless Communications*, vol. 2, no. 6, pp. 1150–1158, Nov. 2003.

[8] J. Li, H. Kim, Y. Lee, and Y. Kim, "A novel broadband wireless OFDMA scheme for downlink in cellular communications," in *Proceedings of the IEEE Wireless Communications and Networking Conference*, 2003, pp. 1907–1911.

[9] G. Song and Y. Li, "Cross-Layer Optimization for OFDM Wireless Networks–Part I: Theoretical Framework," *IEEE Trans. on Wireless Communications*, vol. 4, no. 2, pp. 614–624, Mar. 2005.

[10] H. Kim, Y. Han, and J. Koo, "Optimal subchannel allocation scheme in multicell OFDMA systems," in *Proceedings of the IEEE Vehicular Technology Conference*, 2004, pp. 1821–1825.

[11] Z. Han, F.R. Farrokhi, Z. Ji, and K.J.R. Liu, "Capacity optimization using subspace method over multicell OFDMA networks," in *Proceedings of the IEEE Wireless Communications and Networking Conference*, 2004, pp. 2393–2398.

[12] R. Laroia, S. Uppala, and J. Li, "Designing a Mobile Broadband Wireless Access Network," *IEEE Signal Processing Magazine*, vol. 21, no. 5, pp. 20–28, Sept. 2004.

[13] D. Tse and P. Viswanath, *Fundamentals of wireless communication*, Cambridge University Press, 2005.

[14] A.D. Wyner, "Shannon-theoretic approach to a Gaussian cellular multiple-access channel," *IEEE Trans. on Information Theory*, vol. 40, no. 6, pp. 1713–1727, Nov. 1994.

[15] B.M. Zaidel, S. Shamai, and S. Verdú, "Multicell Uplink Spectral Efficiency of Coded DS-CDMA With Random Signatures," *IEEE Journal on Selected Areas in Communications*, vol. 19, no. 8, pp. 1556–1568, Aug. 2001.

[16] T. Cover and J. Thomas, *Elements of Information Theory*, John Wiley, 1991.

[17] COST Action 231, "Digital Mobile Radio towards Future Generation Systems, final report," Tech. Rep., European Communities, EUR 18957, 1999.

[18] P. Billingsley, *Probability and Measure*, John Wiley, 3rd edition, 1995.

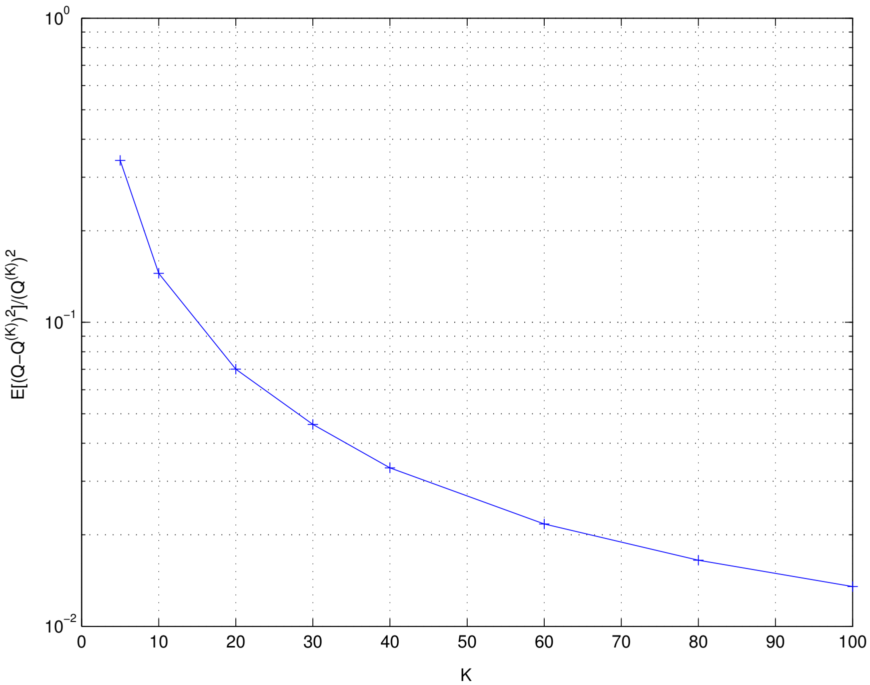

Fig. 3. Single cell context : normalized MSE between the total power Q required by the allocation algorithm and the power required in asymptotic regime $Q^{(K)}$ vs. the number of users K (FSL model)

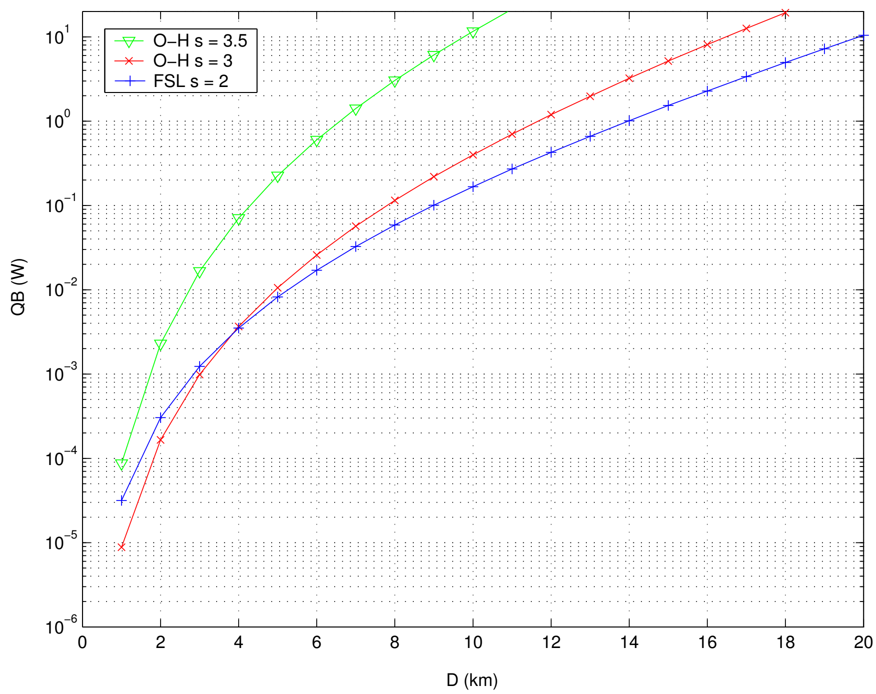

Fig. 4. Single cell context : required power vs. cell radius D, $\overline{r} = 0.2$ bit/s/Hz/km

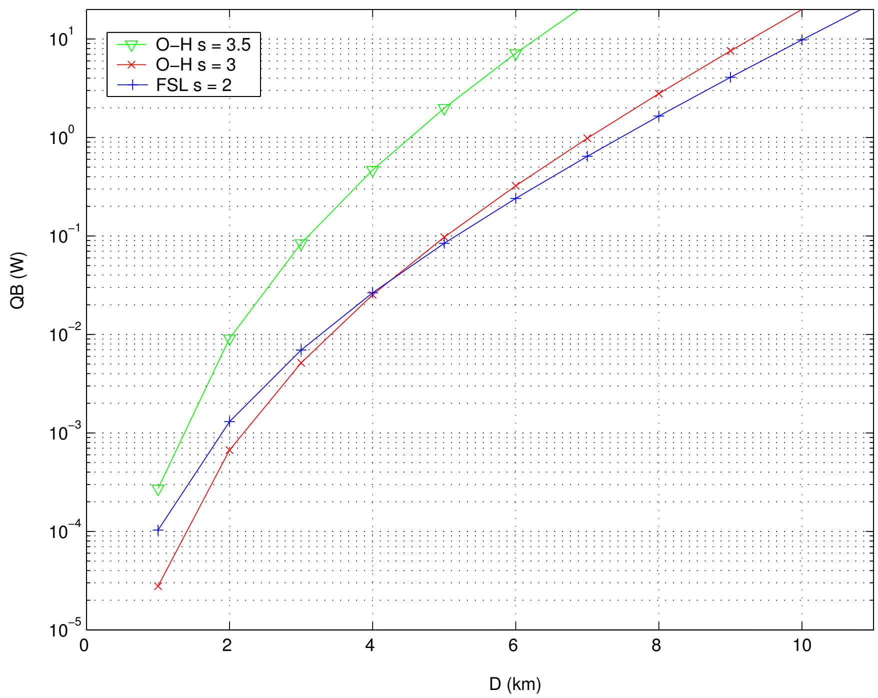

Fig. 5. Single cell context : required power vs. cell radius D, $\overline{r} = 0.5$ bit/s/Hz/km

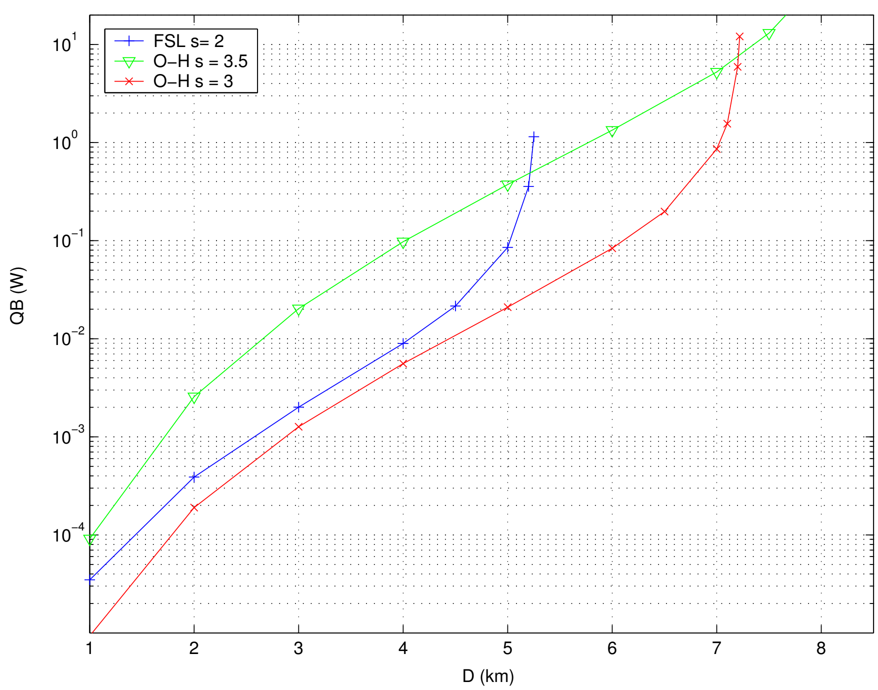

Fig. 6. Multi-cell context : required power vs. cell radius D, $\overline{r} = 0.2$ bit/s/Hz/km

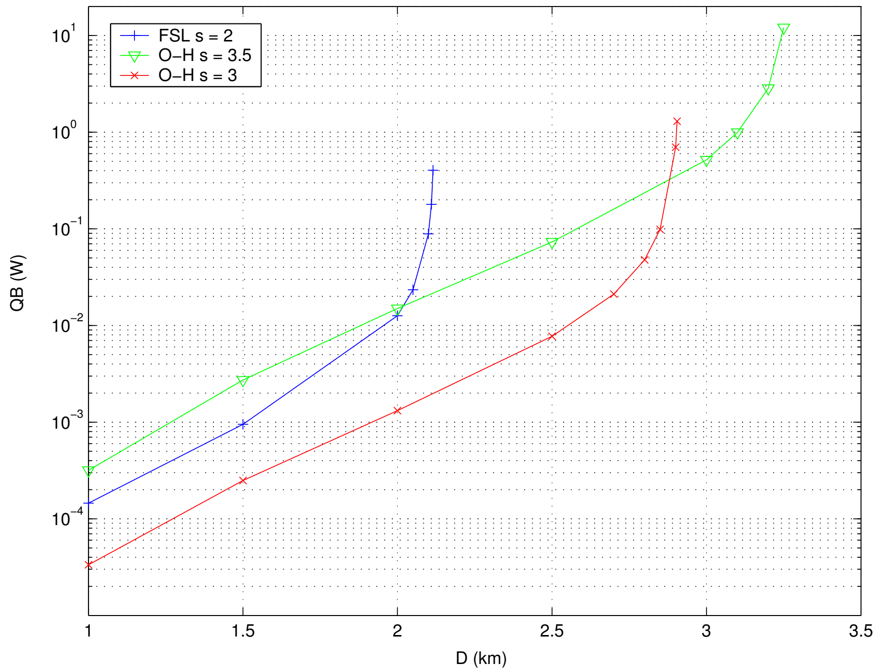

Fig. 7. Multi-cell context : required power vs. cell radius D, $\overline{r} = 0.5$ bit/s/Hz/km

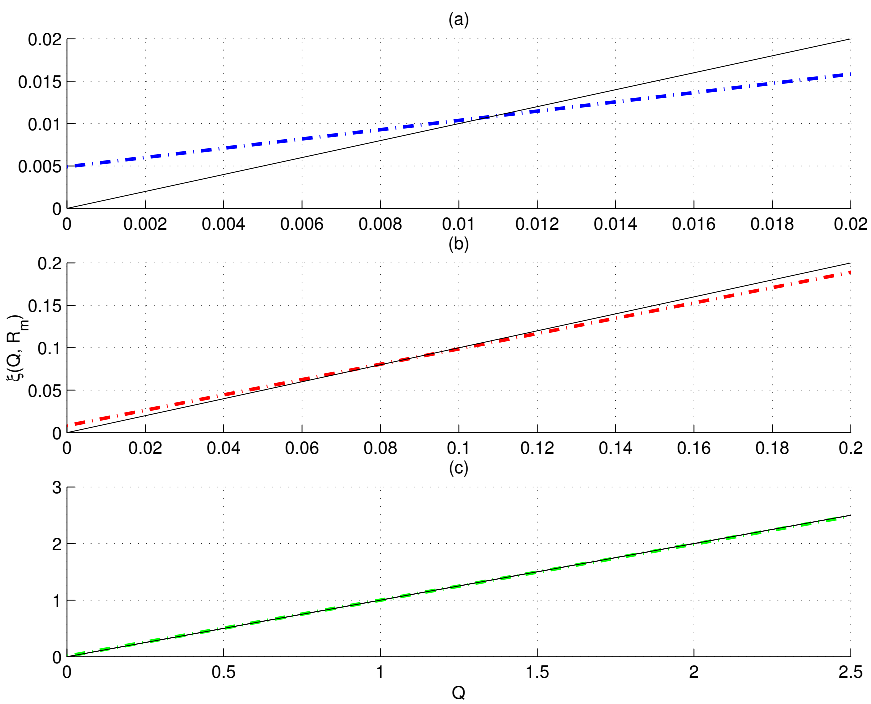

Fig. 8. Function $\xi(Q, \bar{r})$ vs. Q in a 5 km-radius cell for three different mean rate requirements : (a) $\bar{r} = 0.15$ bit/s/Hz/km; (b) $\bar{r} = 0.2$ bit/s/Hz/km ; (c) $\bar{r} = 0.21$ bit/s/Hz/km (FSL model)

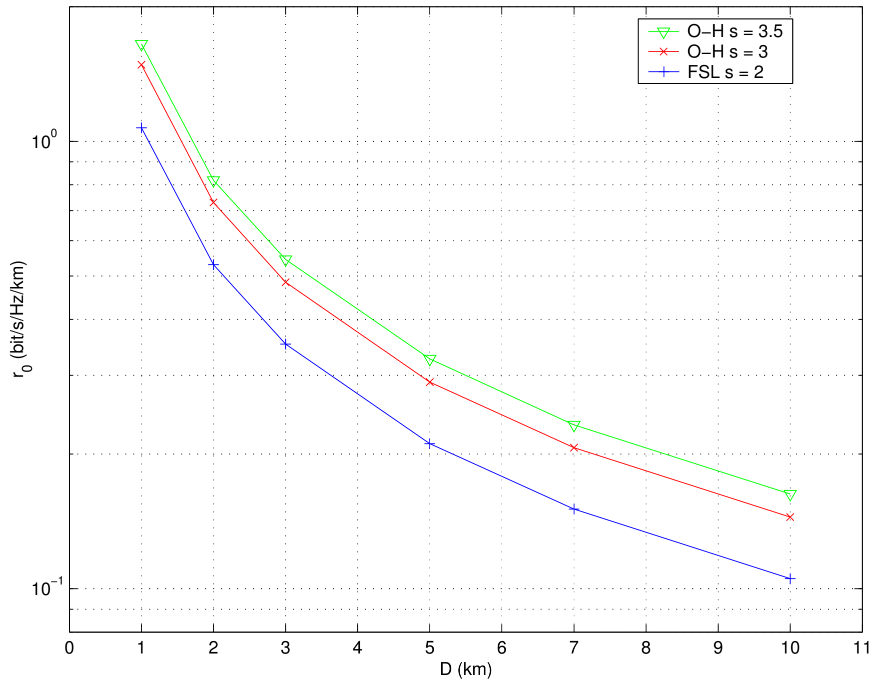

Fig. 9. Limit on the mean rate R_0 vs. cell radius D

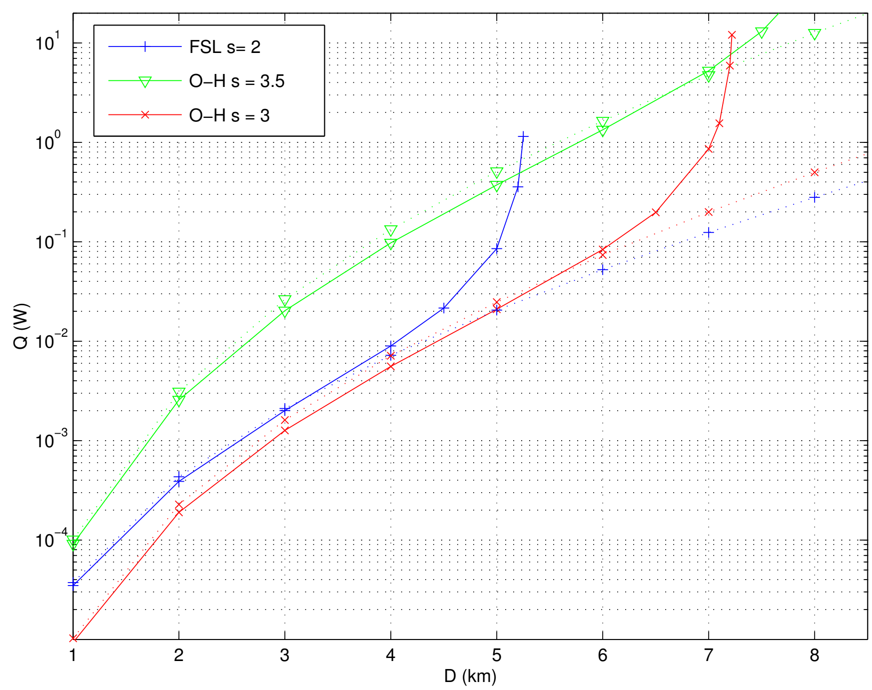

Fig. 10. Power per cell vs. cell size with frequeucy re-use factor equal to 1 (plain) or $1/2$ (dashed).